

***Aquilaria Crassna* Leaves Extracts – a Green Corrosion Inhibitor for Mild Steel in 1 M HCl Medium**

L. Y. S. Helen, A. A. Rahim*, B. Saad, M. I. Saleh, P. Bothi Raja

School of Chemical Sciences, Universiti Sains Malaysia, 11800 Penang, Malaysia.

*E-mail: afidah@usm.my

Received: 24 June 2013 / Accepted: 29 October 2013 / Published: 8 December 2013

The anti corrosion behaviour of agarwood leaves extracts in 1 M HCl solution on mild steel were studied using gravimetric method (weight loss method), electrochemical methods (electrochemical impedance spectroscopy (EIS) and potentiodynamic polarisation) and scanning electron microscope (SEM) techniques. The extracts were shown to have good inhibition efficiencies for the gravimetric and electrochemical methods. EIS analysis revealed that increase in concentration increases the charge transfer resistance, thus increased inhibition efficiency. The potentiodynamic polarisation measurements showed the extracts acted as mixed-type inhibitors with predominantly cathodic effectiveness. SEM techniques supported the success of corrosion inhibition with the presence of inhibitors and the methanol extract best fitted the Temkin adsorption isotherm while the aqueous extract best fitted the Langmuir and Temkin adsorption isotherms. The adsorption mechanisms for both extracts were mainly physisorption.

Keywords: adsorption isotherm, agarwood, *Aquilaria crassna*, corrosion inhibition

1. INTRODUCTION

Corrosion of materials is a natural phenomenon that is a cause of concern as it has incurred a total damage of billions of dollars to many industries. Many ways of overcoming the corrosion problem such as inhibitors, anodic protections, cathodic protections and coatings are developed. Among all the methods, corrosion inhibitors are popular due to the ease in application and the advantage of in situ application without disruption of the process. Corrosion inhibitors are substances which when added in small concentrations to the corrosive environment will reduce the rate of corrosion [1].

Hydrochloric acid is a very commonly used acid but it is one of the most difficult acid to handle due to its very corrosive nature even in dilute forms [2]. Examples of industries using the

hydrochloric acid are the acid pickling industry, industrial cleansing and oil well cleansing. Mild steel is a major construction material that is extensively used in industries that also includes those handling acid, alkali and salt solutions [3].

There has been extensive research done to develop inhibitors that are cost effective and environmentally friendly. Most of the inhibitors developed from natural sources such as plants are found to have the presence of heterocyclic compounds, nitrogen, sulfur and oxygen atoms and these contribute greatly to inhibit ion of corrosion via various mechanisms [4-5]. Examples of plants that had been studied as inhibitors includes *Neolamarckia cadamba*, Mangrove tannins, *Xylopiia ferruginea*, apricot juice, *Zenthoxylum alatum*, *Medicago sativa* [6-11]

Aquilaria crassna or also known as agarwood is from the family Thymelaeaceae. The resin produced from the bark of agarwood tree is used as incense and is highly prized in the perfumery industry for the distinguished scent. The leaves are being processed into teas, used as a digestive ailment and mild sedatives in traditional medicine [12].

Leaves of *Aquilaria malaccensis* has been reported to contain phenolic compounds such as alkaloids, saponins, triterpenoids, tannins and flavanoids in a phytochemical screening which makes it a potentially good inhibitor [13].

In the present study, agarwood leaves extracts was investigated for its corrosion inhibition potential by using weight loss, potentiodynamic measurement, electrochemical impedance spectroscopy and scanning electron microscopy techniques.

2. EXPERIMENTAL

2.1 Extraction

Agarwood leaves were collected from Penang Island, Malaysia and were air dried and powdered. The leaves were extracted exhaustively using methanol at room temperature (27 °C) and was concentrated using a rotary evaporator at 40 °C to yield the first crude extract (ME). Some of the ME extract was dissolved into water, filtered to remove the insoluble residue and partitioned successively with n-hexane, dichloromethane and ethyl acetate. The aqueous layer was then freeze dried to obtain the aqueous extract (AE).

2.2 Chemical analysis

2.2.1 Phytochemical screening

Phytochemical screening of inhibitor samples (ME and AE) were carried out to identify the presence of the chemical constituents; flavonoids, alkaloids, triterpenoids, tannins and saponins. The screenings were done according to methods adopted from Mamta with slight modifications [14].

2.2.2 Total Phenolic Content (TPC)

The TPC was determined using the Folin-Ciocalteu assay, adopted from Kim as mentioned by Tan with slight modifications [15-16]. 0.25 mL of sample or standard diluted in suitable concentration was added into 2.5 mL Folin-Ciocalteu reagent (10% v/v) and left to stand for 5 mins. 2 mL of 1 M Na_2CO_3 was added into the mixture, shaken and incubated at room temperature for 90 minutes. Absorbance was read at 750 nm. TPC value was expressed as gallic acid equivalents (mg of GAE/g sample) using the calibration curve of gallic acid. All the samples were analysed in triplicates.

2.2.3 Total Flavonoid Content (TFC)

TFC of the extracts was determined by adopting the method from Kim as mentioned by Tan with slight modifications [15-16]. 1.0 mL of appropriately diluted sample or standard was added into 4.0 mL distilled water. 0.3 mL of 5 % w/v NaNO_2 was added into the solution and left to stand for 5 minutes. 0.3 mL of 10 % w/v AlCl_3 was added and left to stand for 1 minute after which 2 mL of 1 M NaOH was added into the mixture and diluted with 2.4 mL of water and shaken. Absorbance was recorded at 509 nm and TFC of samples was expressed as (+)-catechin equivalents (mg of CE/g sample). All the samples were analysed in triplicates.

2.3 Fourier transform infrared spectroscopy (FTIR)

ME and AE were screened with FTIR using the Perkin Elmer System 2000. The inhibitor sample was mixed and grounded with potassium bromide (KBr) with the ratio of 1:20 and compressed as a pellet. The spectra were recorded in the range of 4000 to 400 cm^{-1} .

2.4 Corrosion inhibition studies

2.4.1 Sample preparation

Mild steels of the composition by weight percent; 0.039 % P; 0.06% Si; 0.55% Mn; 0.205% C; Fe balance, was used for this study. The mild steels were cut to suitable sizes and polished successively with grade 400, 800, 1200 emery paper, rinsed with double distilled water and then acetone (AR grade) to remove grease. The mild steels were dried at room temperature (27 °C). 1 M HCl was prepared by dilution from 37 % HCl (AR grade) with double distilled water.

2.4.2 Weight loss method

Mild steels of 30 mm × 10 mm × 0.5 mm were weighed for the initial weight. Inhibitors were diluted to suitable concentrations using 1 M HCl. The mild steel plates were further immersed in the solutions at room temperature. After 24 hours of immersion, mild steel plates were removed, cleaned

with distilled water and dried at room temperature. The final weight of the mild steels were recorded. The experiment was repeated in triplicates to check the reproducibility of results. The percentage of inhibition efficiency is calculated using the following formula:

$$IE \% = \frac{W_{(o)} - W_{(i)}}{W_{(o)}} \times 100 \quad (1)$$

Where;

$W_{(o)}$ = average weight loss without the inhibitor

$W_{(i)}$ = average weight loss with the inhibitor at the said concentration

2.4.3 Electrochemical measurements

Electrochemical were carried out using Gamry Instruments reference 600 (potentiostat/galvanostat/ ZRA). Mild steel plates with an exposure area of 3.142 cm² was used as working electrode, platinum electrode (Pt) as the auxiliary electrode while the saturated calomel electrode (SCE) was used as the reference electrode. All the electrochemical studies were carried out at room temperature (27 °C). The open circuit potential (OCP) was recorded as a function of time up to 30 minutes.

2.4.3.1 Electrochemical impedance spectroscopy (EIS)

EIS measurements were carried out at the corrosion potential (E_{corr}) with frequency from 100 000 to 0.1 Hz at amplitude of 10 mV and scan rate of 10 points per decade. The results were represented in Nyquist diagrams and the electrical equivalent circuit for the system were obtained along with the charge transfer resistance (R_{ct}) value. The IE % can be calculated using the following formula;

$$IE \% = \frac{R_{\text{ct}(i)} - R_{\text{ct}(o)}}{R_{\text{ct}(i)}} \times 100 \quad (2)$$

Where;

$R_{\text{ct}(o)}$ = charge transfer resistance of mild steel without the inhibitor

$R_{\text{ct}(i)}$ = charge transfer resistance of mild steel with the inhibitor at a certain concentration

2.4.3.2 Potentiodynamic polarisation measurement

The Tafel polarisation curves were obtained by scanning the electrode potential from -300 mV to 300 mV from the E_{corr} with a scanning rate of 1 mVs⁻¹. The linear segments of the anodic and cathodic curves were extrapolated to E_{corr} to obtain the corrosion current densities (I_{corr}). The IE % can be calculated using the formula:

$$IE \% = \frac{I_{\text{corr}(o)} - I_{\text{corr}(i)}}{I_{\text{corr}(o)}} \times 100 \quad (3)$$

Where;

$I_{\text{corr}(o)}$ = corrosion current density of mild steel without the inhibitor

$I_{\text{corr}(i)}$ = corrosion current density of mild steel with the inhibitor at a certain concentration

2.5. Scanning electron microscopy (SEM)

FEI QUANTA PEG 60 - scanning electron microscope was used to monitor the surface morphological changes. The mild steels were immersed for 24 hours at room temperature in 1 M HCl solution for blank (absence of inhibitor) and inhibitors in their respective concentrations that exhibited the highest IE for weight loss method. Mild steel plates were then rinsed with distilled water and allowed to dry at room temperature and analysed for SEM.

3. RESULTS AND DISCUSSION

3.1 Chemical analysis

3.1.1 Phytochemical screening

Table 1. Result of phytochemical screening

Extract	Alkaloid (Mayer's test)	Flavonoid (alkaline reagent test)	Triterpenoid (Salkowski's test)	Saponin (froth test)	Tannin (FeCl ₃ test)
ME	+	++	+	+	++
AE	+	++	+	++	++

(Where; + represents the weak presence of tested phytochemical, ++ represents the moderate presence of tested phytochemical.)

Phytochemical screenings were done to identify the presence of the chemical constituents (alkaloids, saponins flavonoids and tannins) which are believed to contribute to corrosion inhibition by physical adsorption [17]. The screenings performed is a form of qualitative test. While it cannot determine the phytochemicals quantitatively, it allows for appropriate comparison of one extract to another and is shown in Table 1. The extracts gave slightly more prominent colours for the outcome of the flavonoid and tannin tests indicating it has a moderate amount of the tested compounds present. There was a weak presence of creamy white precipitate for the alkaloid test for both extracts indicating a weak presence of alkaloids. Result for triterpenoid test indicates there was a weak presence of triterpenoids in both extracts. AE produces more froth for the froth test indicating a higher presence of saponins compared to ME.

3.1.2 Total phenolic content (TPC) and total flavonoid content (TFC)

Table 2. Result of TPC and TFC

Extract	TPC (mg gallic acid equivalents/g)	TFC (mg (+)-catechin equivalents/g)
ME	139.21	32.85
AE	184.15	28.62

The TPC and TFC values of ME and AE were presented in Table 2. The phenolic group has –OH as one of the functional groups and will most likely contribute to corrosion inhibition. Examples of phenolic groups that are known to be present in green inhibitors are flavonoids and tannins [18-19]. Flavonoids contribute to the inhibition efficiency of the inhibitors possibly due to flavonoids being cyclic compounds with O atoms attached to it. TPC value for ME is lower than AE but the TFC value of ME is higher than AE. Flavonoids are also phenolic compounds and therefore TFC is expected to be proportional to TPC. However, the partition using solvents to obtain AE may have removed some flavonoids from AE but concentrated other phenolic compounds in AE thus giving it a higher TPC but lower TFC.

3.2 Fourier transform infrared spectroscopy (FTIR)

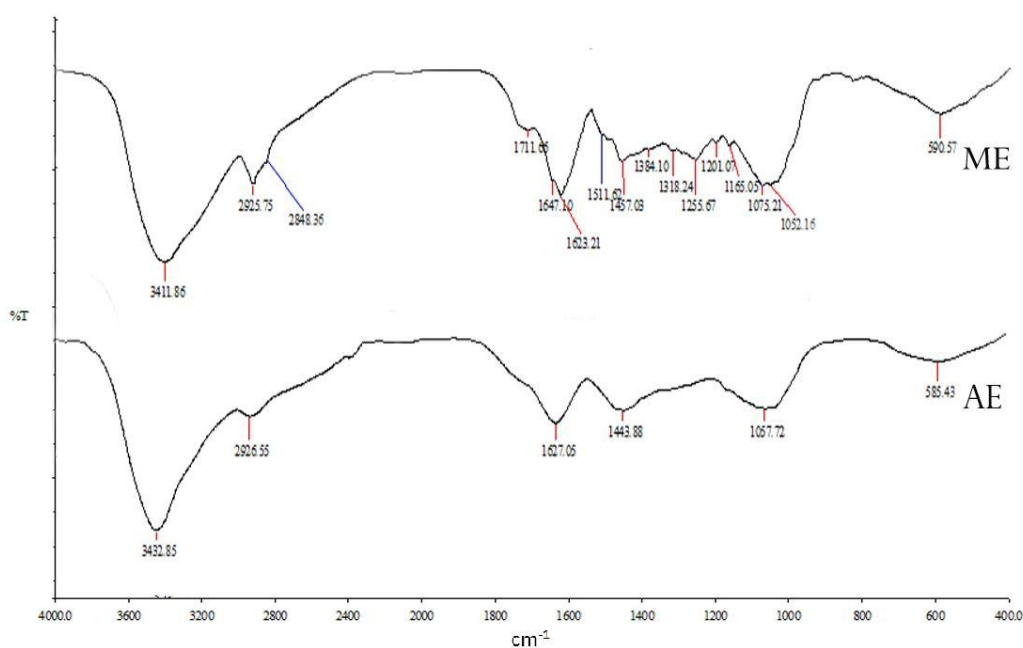


Figure 1. Combined FTIR spectra of *Aquilaria crassna* extracts

The chemical constituents that contribute to the corrosion inhibition have specific functional groups. The inhibitors samples were analysed with the FTIR to identify the functional groups present in the extracts (Figure 1). ME and AE showed strong and broad absorption at 3411 and 3432 cm^{-1} respectively and may be indicating presence of the –OH group. The presence of –NH group in amines should appear in the range of 3500 to 3300 cm^{-1} and may be overlapping with the –OH group in the spectra. The presence of aliphatic stretching of C-H is shown at frequencies 2925 (ME), 2848 (ME) and 2926 cm^{-1} (AE). The C=O group stretching occurs at 1711 cm^{-1} for ME while no absorbance from C=O group is present in the AE extract. The absorbance at 1623 (ME) and 1627 cm^{-1} (AE) indicates the presence of aromatic ring. The presence of C–N stretching of the extracts occurs at 1075 cm^{-1} for AE while no stretching for C–N group was observed for ME extract. From the FTIR spectrum, the ME

and AE extracts may be containing the desirable chemical constituents that are common in good green inhibitors.

3.3 Corrosion studies

3.3.1 Weight loss method

The weight loss method is a form of gravimetric method of studying the anti-corrosion activity of the inhibitors. The results obtained for varying concentrations of the inhibitors are depicted in Table 3.

Table 3. Inhibition efficiencies values of mild steel in 1 M HCl with different concentrations of leaves extracts

Inhibitor	Concentration (ppm)	IE %
ME	0	-
	50	56.13
	100	64.99
	150	66.55
	200	73.73
	250	79.50
	300	80.28
	AE	0
10		20.44
20		32.44
30		49.95
40		61.20
50		68.21
60		69.98

From the Table 3, it is clear that the highest IE % obtained for ME and AE extracts are 80.28 and 69.98 % at optimum concentration of 300 ppm and 60 ppm respectively. The IE % of both extracts increased with the increase of concentrations. This can be explained by the increase of adsorption of inhibitors molecules on the metal and thus increases the degree of surface coverage [20-21]. The increased coverage will protect the metal from the corrosion process as it creates a separation of the metal surface from the aggressor (acid medium).

3.3.2 Electrochemical studies

3.3.2.1 Electrochemical impedance spectroscopy (EIS)

EIS results obtained are given as Nyquist plots (Figure 3 and 4) and were analysed by fitting experimental data into a simple equivalent circuit model shown in Figure 2.

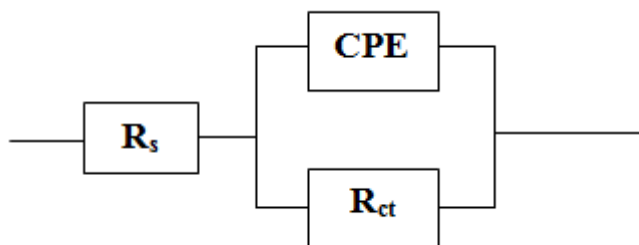


Figure 2. The equivalent circuit model used for obtained Nyquist plots.

Where;

R_s = solution resistance

R_{ct} = charge transfer element

CPE = constant phase element

Various impedance parameters; CPE, n , R_{ct} and IE % were calculated and given in Table 4.

Figures 3 and 4 show the Nyquist plots of mild steels in inhibitors at different concentrations. It was observed that the diameters of the capacitive loops increase with increasing concentration of inhibitors used. This indicates the higher coverage of inhibitors on the metal surface thus increasing the shielding of the surface of mild steel from the corrosive media. This will also increase the resistance towards the electron transfer and thus increases the R_{ct} values. There was no obvious presence of inductive loops indicating the corrosion process is mainly of charge transfer as opposed to iron dissolution [22]. CPE accounts for the surface irregularities and nonuniform distribution of current densities that causes the semicircle Nyquist plots to be depressed instead of the perfect semicircles [23] expected by the EIS theory.

Table 4. EIS parameters of mild steel in 1 M HCl with different concentrations of leaves extracts

Inhibitor	Concentration (ppm)	R_{ct} (ohm. cm^2)	$CPE \times 10^5$ (F cm^{-2})	n (Y_o)	IE %
Blank	0	25.41	12.06	0.9187	-
ME	50	30.52	11.07	0.9145	17
	100	39.65	9.555	0.9159	36
	150	41.54	9.059	0.9147	39
	200	55.78	8.163	0.9107	54
	250	52.98	8.184	0.9126	52
	300	76.36	6.952	0.9079	67
AE	10	42.85	9.465	0.9188	41
	20	46.53	8.922	0.9121	45
	30	47.3	8.68	0.9131	46
	40	58.02	8.139	0.9134	56
	50	62.33	7.573	0.9154	59
	60	52.60	8.341	0.9149	52

The shapes of the semicircles do not change with the increase in concentration suggesting the mechanism of corrosion process did not change with the increase of concentration [24]. The decrease in value of CPE can be attributed to dielectric relaxation and/or increase in thickness of electrical double layer and this increases inhibition efficiency.

The values of n that were almost unchanged account for the non-homogeneity of the metal surface and a closer value to 1 indicates a more homogenous metal surface. It does not account for the physical roughness of the metal surface but can also account for the homogeneity of the electrical layer formed on the metal surface [8].

The IE % were calculated from R_{ct} values and it can be observed that maximum IE % of ME is at 300 ppm (67 %) while as for AE, the maximum IE % is at 50 ppm (59 %). The IE % trend for both extracts is generally increasing, however, the IE % of AE drop after 50 ppm. This might be attributed to optimal potential of AE as a corrosion inhibitor was reached at 50 ppm.

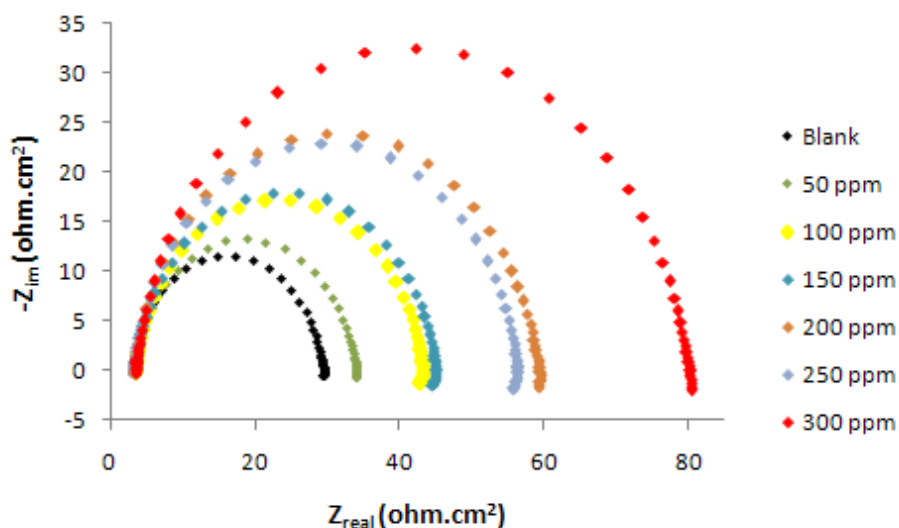


Figure 3. Nyquist plot of mild steel in 1 M HCl with ME at different concentrations

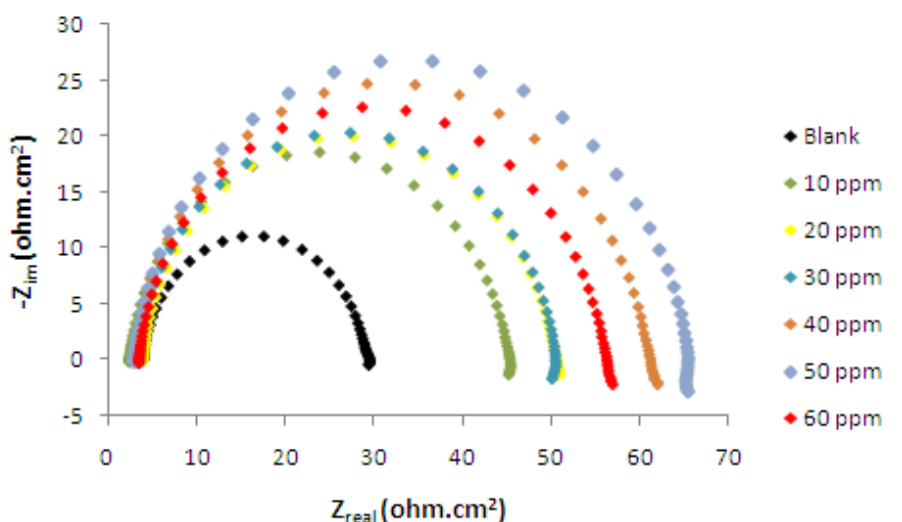


Figure 4. Nyquist plot of mild steel in 1 M HCl with AE at different concentrations

3.3.2.2 Potentiodynamic polarisation measurement

The potentiodynamic polarisation measurement allows for the study of anticorrosion behaviour via anodic and cathodic polarisations. The measurements were recorded and analysed as Tafel plots as shown in Figures 5 and 6 with the electrochemical parameters presented in Table 5. E_{corr} refers to the corrosion potential, I_{corr} refers to the corrosion current density, β_a and β_c refer to the anodic and cathodic Tafel slopes, respectively, of the polarisation curves.

Table 5. Potentiodynamic polarisation measurements parameters of mild steel in 1 M HCl with different concentrations of leaves extracts

Inhibitor	Concentration (ppm)	β_a (mV dec ⁻¹)	$-\beta_c$ (mV dec ⁻¹)	E_{corr} (mV)	I_{corr} ($\mu\text{A cm}^{-2}$)	IE %
ME	0	63	77	-459	859	-
	50	62	71	-459	794	8
	100	55	70	-459	631	27
	150	46	82	-459	501	42
	200	56	97	-460	407	53
	250	41	79	-458	389	55
	300	48	82	-465	282	67
AE	0	61	78	-458	794	-
	10	54	74	-459	631	21
	20	62	78	-467	501	37
	30	54	74	-462	417	45
	40	57	79	-462	398	50
	50	45	75	-459	316	60
	60	43	66	-464	316	60

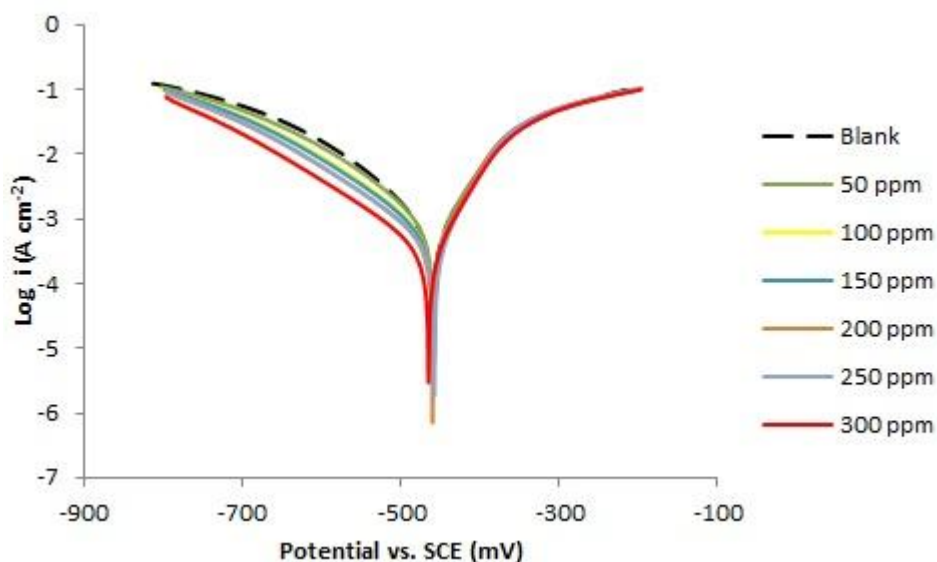


Figure 5. Tafel plot of mild steel in 1 M HCl with ME at different concentrations

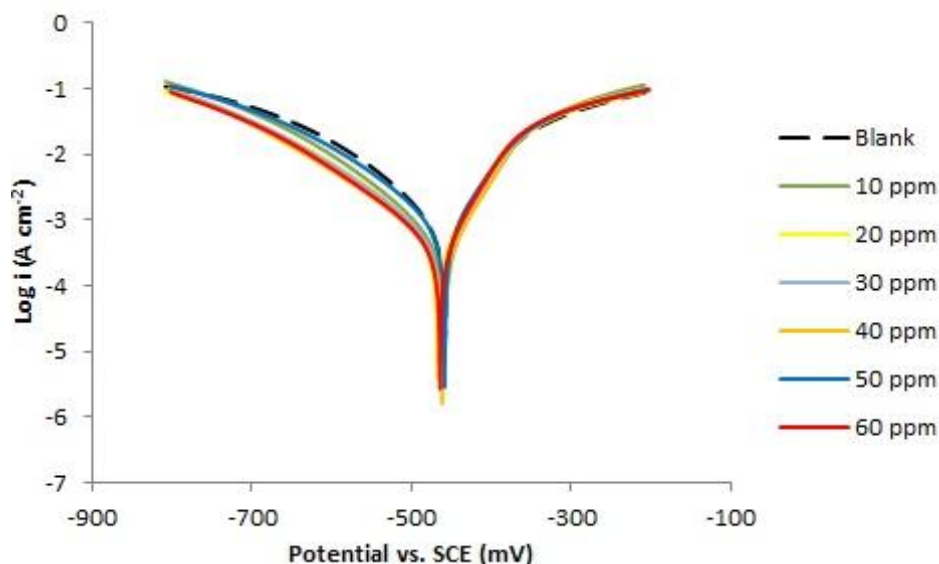


Figure 6. Tafel plot of mild steel in 1 M HCl with AE at different concentrations

The IE %, which was calculated from the I_{corr} , for both extracts reached 67 % and 60 % respectively for the highest concentration of ME (300 ppm) and AE (60 ppm) used. The I_{corr} decreased with an increase of inhibitors concentration for both extracts, increasing the IE % of the extracts as well. The decreasing I_{corr} indicates the success of suppression of corrosion from both metal dissolution and hydrogen evolution on the anodic and cathodic reactions respectively. This is attributed to the increase of adsorption of inhibitors molecules on the metal surface, inhibiting the charge transfer for the anodic and cathodic reaction. An inhibitor can be classified as anodic or cathodic if the displacement of E_{corr} is more than 85 mV with respect to blank [25]. It is evident that for both extracts, both work as mixed-type inhibitors as the E_{corr} displacements were below the mentioned range with respect to blank. The small shifts in β_a and β_c indicates both inhibitors are mixed-type inhibitors [26]. However, β_a recorded higher values than β_c for all concentrations of both extracts. This indicates that the extracts has a higher cathodic current exchange density than its anodic counterpart and works predominantly to reduce corrosion by slowing the cathodic reaction. Both the extracts are therefore mixed-type inhibitors with predominantly cathodic effectiveness.

It can be observed when comparing IE % of ME and AE at concentration of 50 ppm, AE exhibited better IE % than ME for weight loss method, EIS analysis and potentiodynamic polarisation measurement. However, AE faces a limitation when the concentration of inhibitor is increased after 50 ppm as it can also be observed that the IE % at 60 ppm does not increase much for the weight loss method, decreases for EIS analysis and remains plateau for potentiodynamic polarisation measurement. Therefore, AE is a better inhibitor than ME when used at very low concentrations but can only have significant increase in IE % when used up to 50 ppm.

3.4 Scanning electron microscopy (SEM)

Surface morphology of polished mild steel, mild steel immersed in 1 M HCl, mild steel immersed in 1 M HCl with 300 ppm ME and mild steel immersed in 60 ppm AE were recorded and depicted in Figure 7 (a), (b), (c) and (d) respectively. For mild steels immersed in ME and AE respectively, it was observed that there were significant improvements on the surface of mild steels in the presence of inhibitors. The mild steel that was immersed in 1 M HCl (blank) is in a much corroded state compared to the surface of mild steels in the presence of inhibitors. This shows that it could be due to the formation of a protective film by the adsorption of inhibitor on the mild steels thus inhibiting the corrosion.

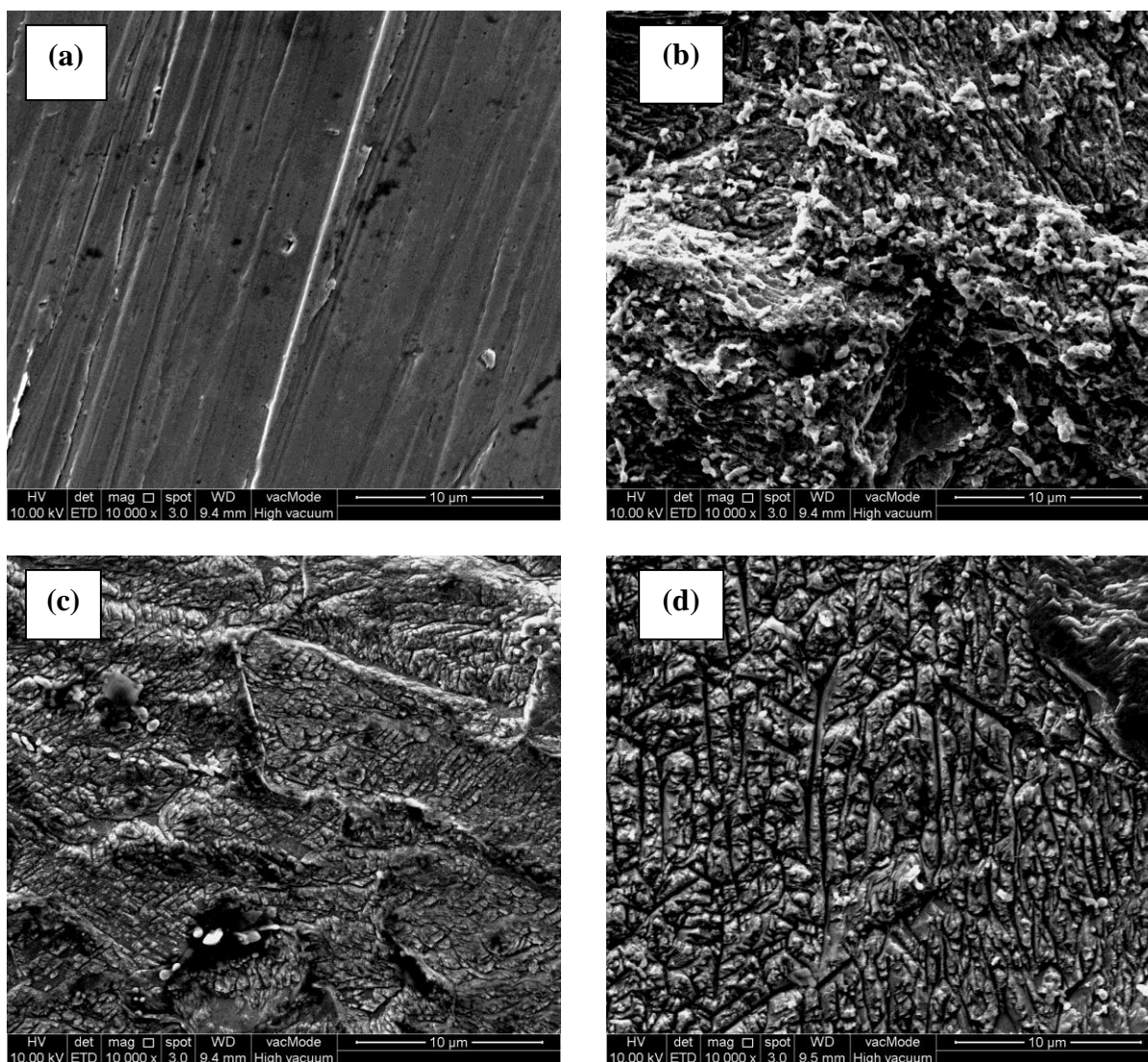


Figure 7. SEM images of mild steel (a) polished mild steel (b) mild steel in 1 M HCl (blank) (c) mild steel in 1 M HCl with 300 ppm of ME (d) mild steel in 1 M HCl with 60 ppm AE

3.5 Adsorption isotherm

The mechanism of the adsorption is further understood by fitting the weight loss method, EIS analysis and potentiodynamic polarisation measurements into adsorption isotherm models. The fit of the adsorption isotherm models are determined by the closeness of linear correlation coefficient (R^2) value to unity. The best fitted models with R^2 closest to unity were then picked to describe the mechanism of adsorption.

The Langmuir adsorption isotherm model assumes that the molecules adsorbed only occupies one site and does not interact with other molecules while Temkin adsorption isotherm assumes molecular interaction between adsorbed molecules [27]. Langmuir model can be represented by equation (4) while Temkin model can be represented by the equation (5):

$$\frac{C}{\theta} = \frac{1}{K_{ads}} + C \quad (4)$$

$$\text{Exp}(-2a\theta) = K_{ads} C \quad (5)$$

Where,

C = inhibitor concentration in g L^{-1}

θ = surface coverage or fraction of inhibition efficiency

K_{ads} = adsorption equilibrium constant

a = parameter of molecules interaction and surface heterogeneity

The K_{ads} is reported to be related to the Gibbs free energy at a single temperature. The value of K_{ads} obtained can be used to calculate the Gibbs free energy via the equation:

$$\Delta G_{ads} = -RT \ln (K_{ads} \times A) \quad (6)$$

Where,

ΔG_{ads} = change in Gibbs free energy

K_{ads} = adsorption equilibrium constant

R = universal gas constant ($8.314 \text{ J K}^{-1} \text{ mol}^{-1}$)

T = absolute temperature (300 K)

A = density of water (1000 g L^{-1})

From the ΔG_{ads} , the type of adsorption can be determined. For values closer to -40 kJ mol^{-1} , the adsorption leans towards chemisorption while for values closer to -20 kJ mol^{-1} , the adsorption leans towards physisorption. The chemisorption phenomenon indicates the occurrence of sharing of electrons or transferring of organic molecule charges with the metal surface while the physisorption phenomenon is attributed to electrostatic interactions between the charged metal and charged molecules [28].

From Table 6, the best fitted adsorption isotherm model for ME is Temkin (Figure 9) and for AE is Langmuir (Figure 8) and Temkin (Figure 10). The ΔG_{ads} values for ME range from -10.15 to $-$

11.93 kJ mol⁻¹ while for AE range from -8.29 to -28.98 kJ mol⁻¹ suggesting the adsorption mechanism of both inhibitors on the mild steel plates is mainly physisorption.

ME and AE are extracted using different methods and thus will contain different organic constituents. The presence of the different compounds contributed to the different trend of IE % as observed from all corrosion evaluation methods for both extracts (ME and AE). As the fit of the extracts to the isotherm adsorption model depends on the trend of the IE % of the extracts, the extracts will then best fit into different adsorption isotherm models, in which ME best fits Temkin while AE best fits Langmuir and Temkin. The adsorption isotherm models describe the mechanism of adsorption of the extracts, where ME fitting the Temkin model implied interactions between adsorbed molecules while AE fitting the Langmuir and Temkin model may be adsorbed by molecules at only one site and does not interact with other molecules (as according to Langmuir adsorption isotherm) or may have interactions between adsorbed molecules (as according to Temkin adsorption isotherm).

Table 6. The values of free Gibbs energy of adsorption calculated from Langmuir and Temkin adsorption isotherm studies on leaves extracts

Adsorption isotherm model	Extract	Method	Slope	Y intercept	R ²	K (L g ⁻¹)	ΔG _{ads} (kJ mol ⁻¹)
Langmuir	AE	Weight loss	0.639	0.043	0.911	23.26	-25.08
		EIS	1.671	0.009	0.966	111.11	-28.98
		Potentiodynamic	1.024	0.035	0.97	28.57	-25.59
Temkin	ME	Weight loss	0.746	1.232	0.987	0.06	-10.15
		EIS	0.609	0.923	0.939	0.12	-11.93
		Potentiodynamic	0.318	0.964	0.953	0.11	-11.69
	AE	Weight loss	0.692	1.557	0.973	0.03	-8.29
		EIS	0.207	0.814	0.716	0.15	-12.55
		Potentiodynamic	0.522	0.973	0.983	0.11	-11.64

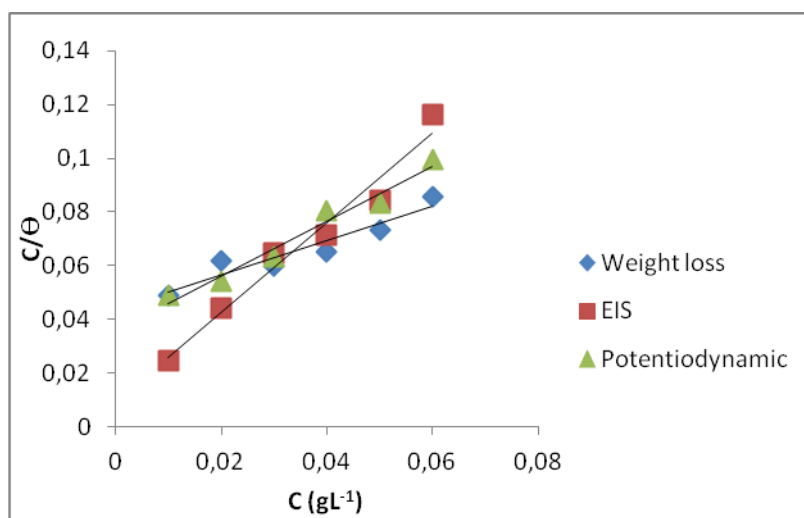


Figure 8. Langmuir adsorption isotherm for AE from weight loss method, EIS analysis and potentiodynamic polarisation measurement

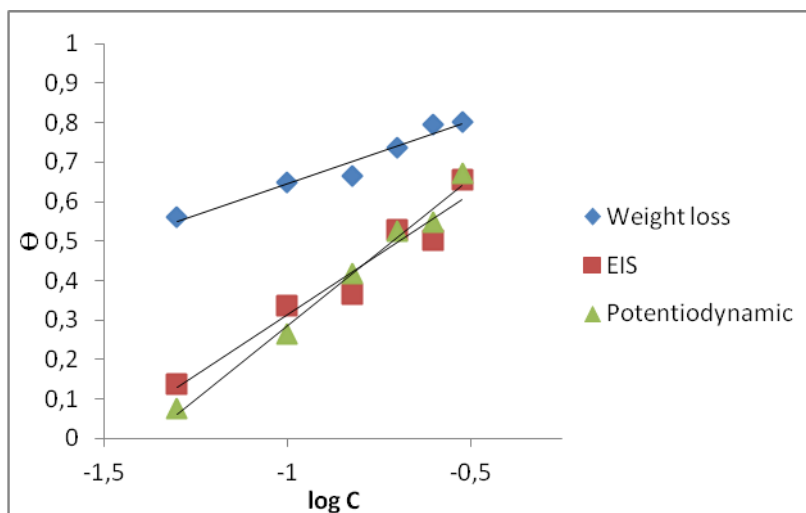


Figure 9. Temkin adsorption isotherm for ME from weight loss method, EIS analysis and potentiodynamic polarisation measurement

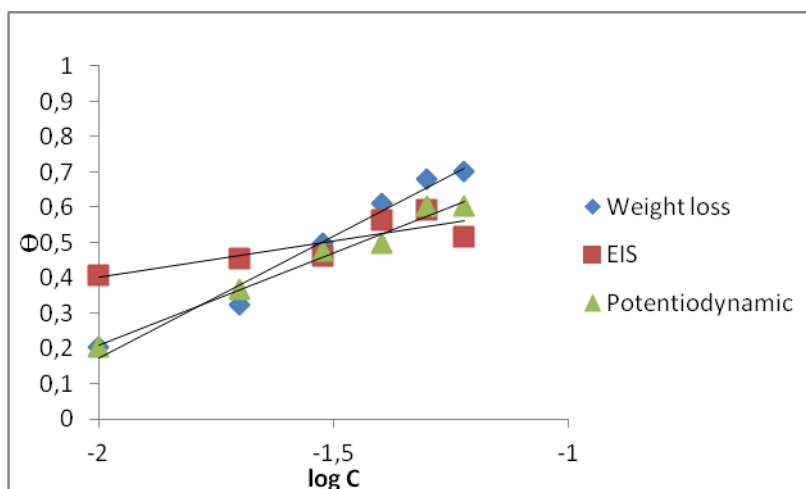


Figure 10. Temkin adsorption isotherm for AE from weight loss method, EIS analysis and potentiodynamic polarisation measurement

4. CONCLUSION

The phytochemical screening confirmed the presence of several important chemical constituents that are related to the anticorrosion properties of the extracts, which was supported by the functional groups detected by FTIR.

From the potentiodynamic polarisation measurements, both inhibitors are mixed-type inhibitors with predominantly cathodic effectiveness. ME better fitted Temkin while AE fitted Langmuir and Temkin adsorption isotherms and the ΔG_{ads} of the inhibitors suggest that the mechanism which inhibitors were adsorbed onto the mild steel surface was mainly by physisorption.

The IE % increases for both inhibitors with the increase of concentration for all anticorrosion behavior measurements. This can be attributed to the increase of inhibitors molecules adsorption onto

the surface of metal thus giving it a protective film from the acidic medium. The presence of the thin protective film is further supported by the SEM surface morphology.

ME shows maximum inhibition efficiency at 300 ppm for weight loss study (80.28 %), EIS analysis (66 %) and potentiodynamic polarisation measurement (67 %) while AE shows maximum inhibition efficiency at 60 ppm for weight loss study (69.98 %) and potentiodynamic polarisation measurement (60 %) but at 50 ppm for EIS analysis (59 %). The inhibition efficiency of AE is as high as ME even when the inhibitor is used at a much lower concentration and this shows that AE is a valuable inhibitor even at very low concentrations.

ACKNOWLEDGEMENTS

The authors are grateful to Universiti Sains Malaysia for the financial support through the completion of this study in the form of Research University (RU) grant (1001/PKIMIA/811213).

References

1. J. O. L. Riggs, Theoretical aspect of corrosion inhibitors and inhibition (First edition), Houston: National Association of Corrosion Engineering (1973).
2. E. A. Noor, A. H. Al-Moubaraki, *International Journal of Electrochemical Sciences*, 3 (2008) 806-818.
3. S.D. Shetty, P. Shetty, H.V.S. Nayak, *Chemical Society*, 71 (2006) 1073-1082.
4. G. Gece, *Corrosion Science*, 50 (2008) 2981-2992.
5. R. A. Prabhu, T. V. Venkatesha, A. V. Shanbhag, G. M. Kulkarni, R. G. Kalkhambkar, *Corrosion Science*, 50 (2008) 3356-3362
6. P. Bothi Raja, A. K. Qureshi, A. A. Rahim, H. Osman, K. Awang, *Corrosion Science*, 69 (2013) 292-301.
7. A.A. Rahim, E. Rocca, J. Steinmetz, M.J. Kassim, R. Adnan, M. Sani Ibrahim, *Corrosion Science*, 49 (2007) 402-417.
8. W.A.W. Elyn Amira, A.A. Rahim, H. Osman, K. Awang, P. Bothi Raja, *International Journal of Electrochemical Science*, 6 (2011) 2998-3016 .
9. A.S. Yaro, A. A. Khadom, R. K. Wael, *Alexandria Engineering Journal*, 52 (2013) 129-135 .
10. G. Gunasekaran, L. R. Chauhan, *Electrochimica Acta*, 49 (2004) 4387-4395.
11. A.M. Al-Turkustani, S. T. Arab, L. S. S. Al-Qarni, *Journal of Saudi Chemical Society*, 15 (2011) 73-82.
12. M. Kakino, S. Tazawa, H. Maruyama, K. Tsuruma, Y. Araki, M. Shimazawa, H. Hara, *BMC Complementary and Alternative Medicine*, 10 (2010) 68.
13. A.W. N. Huda, M.A.S. Munira, S.D. Fitrya, M. Salmah, *Pharmacognosy Research*, 1 (2009) 270-273.
14. S. Mamta, S. Jyoti, *International Research Journal of Pharmacy*, 3 (2012) 5.
15. D-O Kim, S. W. Jeong, C. Y. Lee, *Food Chemistry*, 81 (2003) 321-326.
16. K. W. Tan, M. Jain Kassim, *Corrosion Science*, 53 (2011) 569-574.
17. E. B. Ituen, U. E. Udo, N. W. Odozi, E. U. Dan, *IOSR Journal of Applied Chemistry*, 3 (2013) 52-59
18. S. Martinez, I. Stagljar, *Journal of Molecular Structure: THEOCHEM*, 60 (2003) 167-174.
19. L. A. Nnanna, V. U. Obasi, O. C. Nwadiuko, k. I. Mejuh, N. D. Ekekwe, S. C. Udensi, *Archives of Applied Science Research*, 1 (2013) 207-217.

20. S. Issaadi, T. Douadi, A. Zouaoui, S. Chafaa, M.A. Khan, G. Bouet, *Corrosion Science*, 53 (2011) 1484-1488.
21. A.K. Maayta, N.A.F. Al-Rawashdeh, *Corrosion Science*, 46 (2004) 1129-1140.
22. G. TrabANELLI, C. Monticelli, V. Grassi, A. Frignani, *Journal of Cement and Concrete Research*, 35 (2005) 1804–1813.
23. M. Lebrini, M. Lagrenée, H. Vezin, M. Traisnel, F. Bentiss, *Corrosion Science*, 49 (2007) 2254–2269.
24. M. A. Amin, *Corrosion Science*, 52 (2010) 3243-3257.
25. Y. Yan, W. Li, L. Cai, B. Hou, *Electrochimica Acta*, 53 (2008) 5953-5960.
26. M. A. Quraishi, F. A. Ansari, D. Jamal, *Materials Chemistry and Physics*, 77 (2003) 687–690.
27. S. Paul, B. Kar, *International Scholarly Research Network*, (2012) 2012.
28. G. E. Badr, *Corrosion Science*, 51 (2009) 2529-2536